

The influence of the North Atlantic Oscillation on diverse renewable generation in Scotland

Andrew N. Commin*, Andrew S. French, Matteo Marasco, Jennifer Loxton, Stuart W. Gibb,
John McClatchey¹

Environmental Research Institute, North Highland College, University of the Highlands and Islands, Ormlie Road, Thurso Caithness, Scotland, UK

HIGHLIGHTS

- Strongly positive correlation in October–March between NAO and renewable generation.
- In the highest energy months a positive NAO index increases renewable variability.
- High-energy positive NAO conditions leads to increased wave device cut-outs.

ARTICLE INFO

Keywords:

North Atlantic Oscillation (NAO)
Renewable
Variability
Onshore wind
Offshore wind
Wave power

ABSTRACT

The North Atlantic Oscillation (NAO) is an index measure of the pressure gradient between Iceland and Portugal, with the pressure gradient affecting the strength and track of storms across the North Atlantic and into Europe. This has implications for renewable generation, which are becoming increasingly important with higher renewable penetrations. To explore the impact of the NAO on renewables a hindcast of wave, onshore and offshore wind generation in Scotland was created for the most recent climate normal period (1981–2010).

These hindcast generation figures were compared to NAO monthly index values and showed a strong and significant positive correlation for the high energy portion of the year (October to March). The strength of this relationship is in some instances, most notably for wave generation, weakened by the higher energy positive NAO conditions causing increased device cut-out. The impact of the NAO was also modelled at a seasonal winter scale (December–March) as is usual in NAO analysis. The model showed the strongest influence on capacity factor for offshore wind, with each increase in NAO index of 1 causing a predicted increase of capacity factor of 3.17 (compared to 2.59 for onshore wind, 1.35 for wave, and 2.49 for the combined portfolio). In January and February, the NAO has a statistically significant impact on hindcast generation variability, at a 1–4 h time scale for all resources and 1–24 h timescale for onshore wind and wave, which will have implications for system management.

1. Introduction

Scotland's renewable energy potential allowed the Scottish Government in 2011 to set their ambitious renewable electricity target of generating the equivalent to 100% of Scotland's electricity demand from renewable sources by 2020 [1]. The word equivalent means not all the renewable electricity generated in Scotland will be used there. Therefore, whilst the target is a step forward in terms of renewable penetration it still means fossil fuels will be in the electricity mix. Full reliance on renewable generation for an electricity system is not seen as tenable or desirable by the Scottish Government, due to variability in

renewable generation threatening security of supply. This variability can lead to large inter-annual changes in renewable generation, for example in 2010 the annual capacity factor for onshore wind power in the UK was 21.8% whilst in 2013 it was 28.8% [2].

1.1. The North Atlantic Oscillation

Large climate patterns can drive variation in renewable output on inter-annual scales. The strongest of these in the Northern Hemisphere is the North Atlantic Oscillation (NAO) [3]; which is the primary source of variability for the North Atlantic climate on annual to multi-decadal

* Corresponding author.

E-mail address: andrew.n.commin@gmail.com (A.N. Commin).

¹ Deceased 30th April 2015.

timescales [4–6]. Historically the NAO is defined as an index that measures the difference in surface pressure between Ponta Delgada in the Azores and Stykkisholmur in Iceland [7]; changes in this pressure gradient result in a shift in wind patterns [8]. With a particular correspondence between elevated values of the NAO and strong westerly winds [9]. NAO variations cause significant shifts of air-sea exchanges of heat [10], freshwater [11] and the track of storms and depressions across the North Atlantic Ocean and into Europe [7]. The storm track varies from winter to winter in both its strength and position. A particularly recurrent variation is for the storm track to be either strong with a north-eastward orientation taking depressions into NW Europe (a high NAO winter) [7,12]. Or weaker with an east-west orientation taking depressions into Mediterranean Europe (a low NAO winter) [7,12]; the former resulting in stormier conditions in Scotland, and the latter calmer conditions. Associated with these changes in weather conditions are altering generation levels from weather dependent renewable developments, such as wind farms, having implications for electricity system performance and security of supply.

A study by Curtis et al. [13] found the NAO to have a significant impact on monthly mean wind speeds, wind power output, and consequently carbon dioxide emissions from the entire Irish electricity system. The NAO impact on emissions depended on the level of wind penetration within an electricity system, but the study indicates emissions intensity within the Irish electricity system could vary by as much as 10% depending on the NAO phase within the next few years [13]. Scotland's renewable targets are more ambitious than Ireland's making improved understanding of the potential impacts of the NAO a pertinent issue.

Earl et al. [14] note recent wind industry discussion of the low-wind year of 2010 (which was strongly affected by a very negative NAO) requires further supporting analysis and discussion of the wider context of the NAO. Ely et al. [15] also argue it is important to understand the impact of the NAO on European electricity systems. Recent research by [16] corroborates the impact of the NAO on wind patterns in Scotland. With low-pressure systems between Greenland and Scotland being steered by stronger sea level pressure, occurring during positive phases of the NAO and causing the W-SW winds rise around 60 °N [16].

1.2. Study scope

This study seeks to increase the understanding of the significance of the NAO in the context of a renewable electricity system; going beyond establishing long term links between the NAO and energy influx or examination of one of extreme events (such as the winter of 2009/2010). This is particularly important given recent changes in the NAO, including increased winter variability, observed in recent studies [17]. Scottish renewables are an informative context in which to pursue this increased understanding, due to strong government targets for renewables and, associated with this, large levels of built, consented or leased areas of renewable development. In previous studies focusing on electricity generation and the NAO in northern Europe onshore wind has the resource predominantly explored [13–15,18,19]. In addition to onshore wind this study also examines offshore wind and wave power. Scotland has been a pioneer in this latter and immature technology since Salter's Duck in the 1970s, through to the establishment of the European Marine Energy Centre (EMEC) in 2003, to the world's first commercial scale leases for wave developments in 2010. A recent study notes that since the NAO exhibits considerable inter-annual variability, it is important that this variability is captured by any wave resource assessment in Scotland [20]. Given the current immature state of the industry this variability has only been explored in terms of generating technology on one occasion [21], this study seeks to expand this knowledge base.

Initially this study seeks to examine the relationship between and quantify the impacts of the NAO on renewable generation, on monthly and seasonal scales. There are studies examining onshore wind in this

context, however, we are unaware of studies examining a mixed portfolio such as is done here. Of particular novelty is the inclusion of wave power, whilst other studies have examined links between raw wave characteristics and the NAO (e.g. [22]) this study takes the novel step of applying power matrices for wave technologies which have seen extensive sea trials – to give a better indicator of actual device performance. A further novelty is the wave power modelled is for areas and capacity leased for wave development. Similarly, for onshore and offshore wind only existing, consented or leased wind farms are modelled, further details are provided in Section 2. Consequently, it is possible gain a novel insight into what renewable generation might look like in the next decade in Scotland.

This study also explores the relationship between the NAO and short-term variability of renewable generation (at 1, 4, 12 and 24 h time scale). Understanding these short-term fluctuations is important in designing sustainable energy systems, in order to account for factors such as reserve capacity and ramp up flexibility. Ramping events are recognised as one of the most problematic issues for network operators to manage [23], however, the short term variability which often causes them is underexplored in the context of the NAO. Only one recently published study explores this (for onshore wind in Ireland, which has a lower capacity than Scotland) [23], the greater renewable capacity and diversity modelled within this study aims to improve the understanding of this relationship in a wider renewable context.

A further novelty examined in this study is the relationship between the NAO and renewable shutdown due to high-energy conditions. Whilst it is generally recognised that there is an increase in energy availability in northern latitudes with a positive NAO index, there are not studies questioning whether this additional available energy can be effectively exploited. With new and emerging technologies, like wave harvesters, it is important to establish how effectively devices will function in high energy conditions associated with positive NAO conditions. This is not only for system operators but also device developers and generators, as if devices are unable to function in high energy conditions it can lead to a loss of income. In general, the impact of the NAO on the economics of renewable generation is not well understood [24], to improve this understanding the relationships modelled between the NAO and generation are contextualised in impact upon income.

2. Methodology and study data

Much of Scotland's potential renewable capacity is yet to be built. In order to characterise how such a renewable portfolio would perform hindcasting was utilised; taking historic wind and wave conditions to infer generation for existing and future potential renewable capacity. Data from a 30 year time series (1981–2010) was used in this study, as the World Meteorological Organisation classify this as the most recent climate normal period [25].

2.1. Onshore wind

To hindcast onshore wind, measured wind speeds are preferred to modelled datasets in the UK; e.g. [26–28]. There are two main reasons behind this, Sharpe et al. [29] observe that alternative satellite reanalysis datasets do not perform as well in high wind speed environments in the UK. Secondly, Dragoon [30] notes weather models are more highly correlated in space than actual wind speeds. Given the complex terrain of Scotland could be a potentially major issue, particularly in examining the links between variability of output and the NAO on a fine temporal scale.

2.1.1. Onshore wind data

For this work, data from the Met Office Integrated Data Archive System (MIDAS) was obtained from the British Atmospheric Data Centre's (BADC) website [31]. This data archive uses measurements

from an extensive network of weather stations across the UK, operated by the Met Office.

The data required cleaning, with the removal of repeat recordings for the same hour, removal of incorrect versions of the data, and the insertion of missing time-steps. The insertion of missing time-steps is required as when there is no recording at a MIDAS station the whole hour is missing from the record, with the next time-step only being when the next measurements were recorded. This presents problems for analysis, as datasets are not uniform in length. The addition of missing hours only adds a time measurement; it does not attempt to infill missing wind parameters. This method adds no wind speed, i.e. no generation calculation will be performed, rather than adding a 0 knots wind recording which would result in zero output and have a greater impact on analysis. The records of MIDAS stations taking wind measurements in Scotland vary greatly in length and quality. All MIDAS stations experience times when no recording is taken (due to factors like instrument failure), leaving gaps in the data set. There is a large disparity in the prevalence and extent of these missing records at different stations; < 1% in some instances and > 10% in others. Details of the occurrence of missing values in the MIDAS stations used to model wind output is provided in Table 1.

From the cleaned MIDAS data, the suitability of stations for use in the study was assessed on: record length (long records were preferred but in one instance only a 12 year record was available), the number of missing wind speed and direction measurements (if > 6% of values were missing a station was rejected), and the proximity of the station to wind farms. For all but one wind area (that modelled using the Leuchars MIDAS station) all wind farms were within 65 km of the MIDAS station. The Leuchars MIDAS station, by Scottish standards, is in an area of not very complex terrain. The land is low lying, with any slopes being very shallow and although there is a small urban and wooded area within relatively close proximity, the station is on an airfield meaning the immediate surface roughness is consistent and low. Given these factors and to enable large wind farms to be modelled, which would otherwise have to be excluded, it was considered acceptable to model wind farms of nearly 80 km distance from the Leuchars MIDAS station.

Records were also examined for other abnormalities, including unusually large numbers of calms. Using these criteria 16 MIDAS stations were selected (a similar number to other studies when characterising Scottish onshore wind, e.g. [26–28,32,33]) for wind farm modelling, detailed in Table 1 with their location provided in Fig. 1. These criteria led to the exclusion of Strathallan Airport (MIDAS station

Table 1

Details of MIDAS stations used for wind modelling. The wind capacity represented is either built, under construction or accepted as of June 2012. Missing values refer to if either the wind speed or direction, or both, are missing – as both elements are required for calculating wind farm generation.

Station name	MIDAS station ID	Length of record (years)	Missing values (%)	Average wind speed (m/s)	Wind capacity represented (MW)
Aviemore	113	28	3.08	3.59	191
Charterhall	268	23	3.60	4.39	528.96
Dunstaffnage	918	30	2.72	4.23	133
Dyce	161	30	5.23	4.55	156.9
Eskdalemuir	1023	30	0.55	3.69	660.4
Kinbrace Hatchery	48	12	1.10	3.94	213.5
Kinloss	132	30	0.09	4.64	257.6
Lerwick	9	30	0.39	7.48	379
Leuchars	235	30	0.72	4.85	323.2
Loch Glascarnoch	67	19	3.59	4.52	208.1
Lossiemouth	137	30	0.26	5.15	286.95
Machrihanish	908	30	1.79	6.23	125.45
Salsburgh	982	30	2.88	6.48	1033.35
Stornoway Airport	54	30	1.00	5.96	272.15
West Freugh	1039	30	0.51	5.18	669.9
Wick Airport	32	30	2.46	5.69	339.3

212) and its replacement with Leuchars (235). Strathallan Airport had the highest percentage of calms in any of the MIDAS records examined (19%) whilst for the stations used the highest proportion of calms was less than 5%.

The majority of MIDAS stations used are in exposed areas, so as not to bias a particular wind direction or wind speeds. However, given the topography of Scotland this is not always possible. Some stations are in valleys or in the lee of large topographic features. Aviemore is the most strongly impacted by this, with the MIDAS station being located in a very steep sided valley, which acts to channel winds in a northeast–southwest direction.

The wind capacity listed in Table 1 is not evenly distributed within Scotland, this is illustrated in Fig. 1.

In this study only onshore wind farms which are either operational, under construction, or consented as of June 2012 are considered, the location of the wind farms modelled is displayed in Fig. 1. Many of the wind farms either in planning or scoping, and thus omitted, are in areas which already have significant wind development, such as in Southern Scotland in Dumfries and Galloway. The wind farms used will therefore be representative of future wind farm installations.

The only area with large wind developments not modelled or mapped in Fig. 1 is the Isle of Skye, which has 69 MW of installed capacity. The mountainous terrain of the island necessitates wind measurements to be made close to the wind farms, as the nearest suitable MIDAS station was on the mainland the error this would create was considered to be too high.

Small wind farms and individual turbines are not included as it is a very intensive process to integrate these developments. Orkney, which has the highest density of such developments, has a collective wind capacity of 45.75 MW, which is a very small share of overall wind portfolio modelled – 0.79%. Exclusion of developments such as those on Orkney thus makes negligible difference to Scotland's wind output on a national scale.

2.1.2. Onshore wind farms

Only onshore wind farms which are either operational, under construction, or consented as of June 2012 were considered (Fig. 1); this totals 5779 MW.

2.1.3. Modelling onshore wind generation

The Wind Atlas Analysis and Application Program (WAsP) was used to extrapolate wind data from the measured MIDAS stations to wind farm locations for the 30 years of MIDAS data. Other authors have used WAsP for similar applications e.g. [27,28,32,34], although typically not for specific wind farms.

The local wind climate of an area depends on its topography [28], thus robust application of WAsP requires detailed topographic data. In this work orographic data used was UK Ordnance Survey 'Profile', which provides contours at 1 and 10 m intervals, depending on terrain (with extreme heights in terrain being measured to the nearest 1 m). This fulfills the criteria for accurate use of WAsP in complex terrain described by [35].

The European land cover database 'Corine Land Cover 2006' [36] is a suggested source of information for surface roughness in WAsP [37] and was used in this study. The 100 m resolution of the dataset falls between the original Corine dataset which has a 250 m resolution and Landsat data which has a 20 m resolution, both datasets were criticised by [38] for being too coarse and too fine respectively.

WAsP can also take into account the wake effect of wind turbines, if their individual coordinates within a wind farm are available. These data were used for the wind farms in this study; being gathered from the developers themselves, the Ministry of Defence, and Scottish Natural Heritage.

To account for downtime a 2.5% loss was applied to the hourly data in the output chronologies created using WAsP [39–41]. The electrical loss within the wind farm was calculated in the same way, after losses

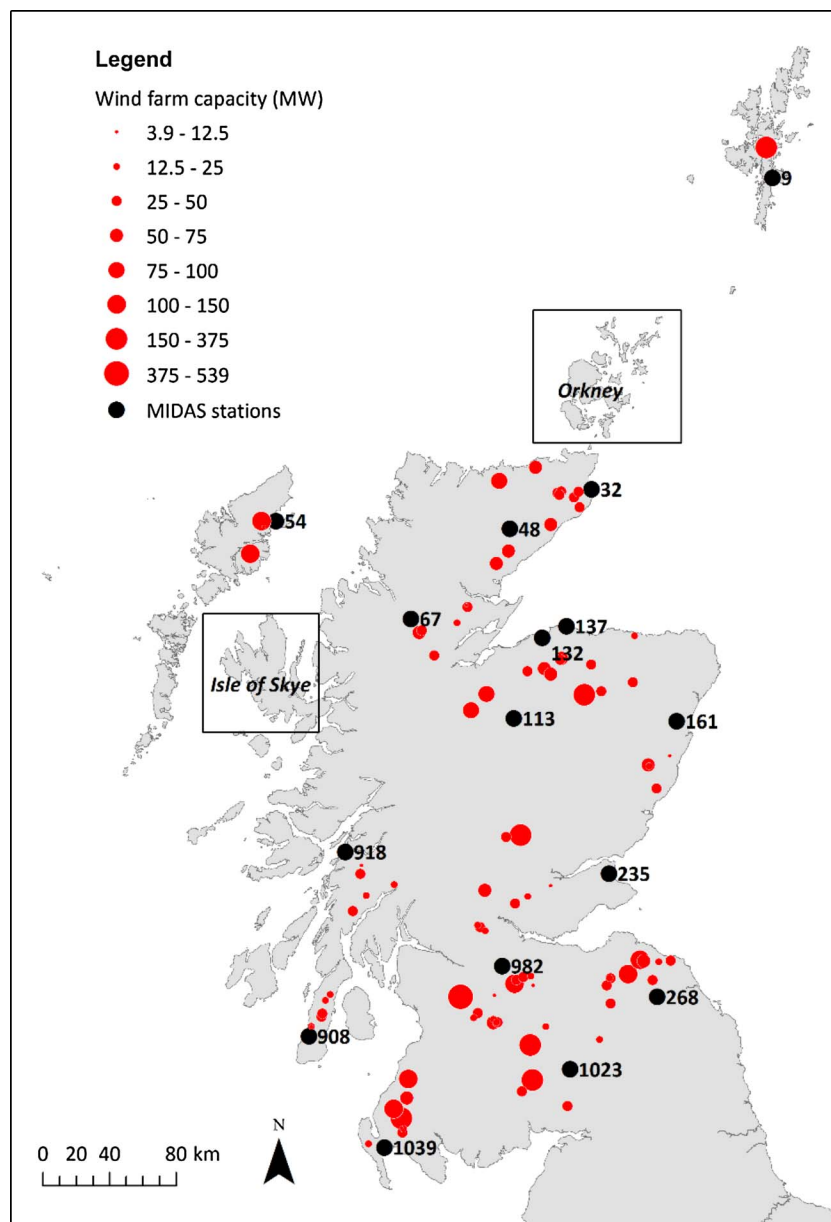


Fig. 1. Wind farms modelled and MIDAS stations used (text next to MIDAS stations indicates station ID). Crown copyright ©.

due to downtime were accounted for. The level of electrical loss was taken to be 3%, in accordance with the upper end electrical losses identified by [39,41].

2.2. Offshore wind

As extended and extensive wind records are not available for offshore conditions modelled data is needed for the hindcasting process.

2.2.1. Offshore wind data

NASA's Modern-Era Retrospective Analysis for Research and Applications (MERRA) was the chosen modelled dataset. MERRA is downloadable from NASA [42] with details of the model provided in [43]. MERRA was generated with the Goddard Earth Observing System (GEOS) atmospheric model and data assimilation system (DAS), and covers the modern satellite era from 1979 to present [44]; thereby covering the full 30 years of this study. GEOS-DAS implements incremental analysis updates to slowly adjust the model states towards the observation state and provides hourly data on a $0.5^\circ \times 0.667^\circ$ grid (equating to approximately $28 \text{ km} \times 74 \text{ km}$ grid in our study region).

The superiority of these temporal and spatial resolutions to other data sources, such as the European Centre for Medium-range Weather Forecasts ERA Interim model (which provides three hourly data on a 0.75° longitude/latitude grid), made it the most suitable data source for this analysis.

A large validation study for MERRA has been carried out by the Crown Estate using 25 different stations in UK waters [45]. The results show good correlation between modelled and measured data; R^2 values of 0.9 or greater for daily correlations [45]. The correlation improves in conditions further from shore, and all offshore wind farms in this study fall within what would be considered as better correlation conditions.

The good match between the MERRA and measured wind data is due to the lack of terrain and a consistent surface type. Consequently, there are not large errors caused by the coarse resolution and parameterisations inherent to model data.

Wind data from MERRA is provided in the form of U (east-west) and V (north-south) wind components. For use in WAsP, data were converted to a direction (degrees) and a wind speed (m/s) format. Wind speed is calculated as [46]:

$$\sqrt{(U \times U + V \times V)} \quad (1)$$

and wind direction as [47]:

$$180 + (180 \div \pi) \times \arctan(V, U) \quad (2)$$

The wind data calculated in this way was taken for three MERRA grid points, to represent the three major areas of offshore wind development in Scotland (described in Section 2.2.1.): 58 °N/2.6667 °W to represent the Moray Firth area, 56.5 °N/1.3333 °W for the Firth of Forth, and 55 °N/2.6667 °W for Islay.

2.2.2. Offshore wind farms

As of 2013 the Crown Estate offshore wind leases fell into three main areas: Islay (the smallest area containing one 680 MW); the Firth of Forth (with three leases – the Forth array with 3500 MW, Inch Cape adds a further 905 MW, and Neart na Gaoithe 450 MW); and the Moray Firth (containing the 920 MW Beatrice and the 1300 MW Moray Firth leases) [48]. With the exception of the Neart Na Gaoithe wind farm, details of the prospective turbine layout were not available. In the case of the other five wind farm leases ArcGIS was used to drape a 1.3 km × 1 km grid over the area leased by the Crown Estate. The grid is not square as the turbine spacing in the Neart Na Gaoithe array suggests this rectangular configuration is more suitable. The coordinates of the centre points of this grid were extracted to provide a theoretical turbine layout. This approach is justified by the low turbine density in this study, which means there is negligible difference between a standard grid layout and location specific siting of turbines [49].

A low turbine density is afforded by the large areas covered by the leases. In some cases, most notably the Firth of Forth and Moray Firth arrays, the size of the lease greatly exceeds the area needed for the turbine spacing assumed in this study (in the Forth Array only 583 turbine locations were required but the methodology created over 2000 possible locations). In these cases turbine locations were selected to fulfil three criteria: areas which are indicated to be first developed (which is the case of the Forth Array) are selected preferentially, locations are as close to land as the lease allows, and the turbine locations selected are closely bunched. Being close to land and turbine bunching was assumed to be favourable to minimize installation, maintenance and transmission costs.

There was a lack of detail available on turbine type for offshore wind development and few power curves and power coefficients available for offshore wind turbines both within WAsP and in the public arena. In WAsP the newest offshore wind turbine available to model is the Vestas V112 3 MW which is considerably smaller than the 5–10 MW offshore wind turbines likely to be seen in Scotland. Using the turbine editor program in WAsP, and specific cut-in and cut-out speeds, rotor diameter, hub height, the thrust coefficient curve and the power curve, ‘model’ turbines were created.

Siemens provides the cut-in and cut-out speeds, rotor diameter and hub height for a 6 MW offshore turbine (Siemens, 2014); and Vestas provide the same information for their V164 8 MW turbine (Vestas, 2013). The cut-in speed for the V112 turbine is 1 m/s slower than that of the larger turbines, at 3 m/s as opposed to 4 m/s and so forth (although the cut out speed was kept at 25 m/s). As a result, the power output for V112 at 3 m/s was taken to be proportionate, in terms of turbine capacity, to the output of the larger turbines at 4 m/s. Similarly, the thrust coefficient for the larger turbines is taken as that experienced for wind speeds, 1 m/s lower in the case of the V112. The theoretical curves, which are used in this study, created from the V112 information and these assumptions are displayed in Fig. 2.

2.2.3. Modelling offshore wind generation

The WAsP model was also used to hindcast wind in an offshore context, using the same methodology described in Section 2.1.3. This offshore application of WAsP has been established as suitable in

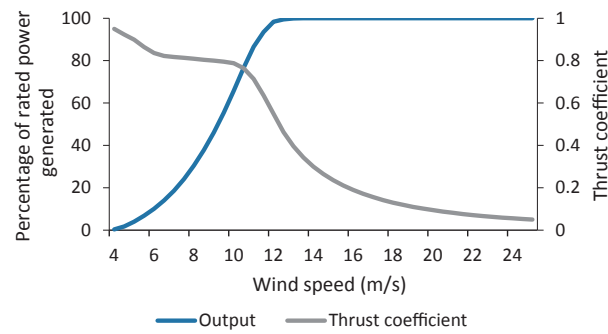


Fig. 2. Thrust coefficient and power curve for the theoretical offshore turbines (6 MW and 8 MW) used in this study.

previous studies [50–52]. To the hourly output figures an electrical loss of 3% and a transmission loss of 3% were applied [40,53].

2.3. Wave

Wave power is the least mature of the three renewable technologies examined. The majority of the potential wave developments hindcast in this study come from the Crown Estate's 2010 leasing round, which represented the first commercial scale leases for wave generation in the world. The number of leases was expanded to a total of 660 MW capacity by 2013, all based around Scotland's north and west coasts where the wave energy is highest [48,54].

2.3.1. Wave data

In the UK there is a lack of suitable measured wave data for use in this study, both in terms of record length and measurement locations; consequently, modelled data from the European Centre for Medium-range Weather Forecasting (ECMWF) was used. This reanalysis model assimilates data from many sources including weather balloons and surface records from stations and ships but the majority of the data originates from satellites [55]. Extensive details of the theory behind the model are provided by the ECMWF [56].

The ECMWF wave model describes the rate of change of the 2 D wave spectrum in any water depth, caused by wind, advection, white-capping, bottom friction, and non-linear wave interactions [57]. Wave height data are assimilated from satellites [57]. Days are split into four periods by the model, with data being provided for 0000 (UTC), 0600 (UTC), 1200 (UTC) and 1800 (UTC) [58]. These periods do not represent an average for the surrounding hours; instead data is valid for the given time. The model data is represented by the centroids of a 0.75° latitude/longitude Gaussian grid.

Given the northerly location of the points of interest a latitude/longitude grid results in some distortion, this provides an east/west resolution approximately twice as fine as that of the north/south. This distortion in favour of the east/west resolution is preferable; as the Atlas of UK Marine Renewable Energy Resources suggests that an east/west difference in location is more important than a north/south one in terms of wave energy (ABP, 2008). This is due to the reduction in available energy as land is approached due to shallower waters.

With the exceptions of the South West Shetland site (where an ECMWF data point falls within the leased area) and the Farr Point site, the wave parameters for each potential wave farm were determined using more than one ECMWF data point. This enabled the six hourly wave data for the array to be weighted appropriately to location. Sites were weighted in direct proportionality to distance; details of this are provided in Table 2.

Determining the wave parameters of arrays using multiple data points provides a more realistic account of any geographical wave farm smoothing. If the closest data point to the lease was to be used, all four of the leased sites in Lewis would have the same wave parameters for

Table 2

Arrays and the ECMWF data point used to generate wave device output.

Wave lease	ECMWF data points used (latitude/longitude)	Weighting of points
Brough Head	59.25 °N/3.75 °W and 59.25 °N/3 °W	0.479:0.521
Costa Head	59.25 °N/3.75 °W and 59.25 °N/3 °W	0.379:0.621
Farr Point	58.5 °N/4.5 °W	1
Marwick Head	59.25 °N/3.75 °W and 59.25 °N/3 °W	0.521:0.479
West Orkney Middle South	59.25 °N/3.75 °W and 59.25 °N/3 °W	0.543:0.457
West Orkney South	59.25 °N/3.75 °W and 59.25 °N/3 °W	0.551:0.449
Bernera	58.5 °N/7.5 °W, 58.5 °N/6.75 °W and 57.75 °N/7.5 °W	0.366:0.401:0.233
Galson	58.5 °N/6.75 °W and 58.5 °N/6 °W	0.629:0.371
North West Lewis	58.5 °N/6.75 °W and 58.5 °N/6 °W	0.657:0.343
South West Shetland	60 °N/1.5 °W	1

any given time, as would four of the five Orkney sites.

2.3.3. Adjusting wave data

The ECMWF model provides three wave parameters: mean wave direction, mean wave period (Mwp), and significant height of combined wind waves and swell (Hs). Ideally, for calculating device output, the energy period (Te) would also be available. Te is the mean wave period with respect to the spectral distribution of energy. The best way to consider Te is as the period of the regular wave during the sea state at the time, whereas Mwp is calculated using the reciprocal moment of the frequency spectrum [59]. Te was calculated from Mwp using the same methodology as the UK Marine Energy Atlas. For the Marine Energy Atlas a standard JONSWAP (Joint North Sea Observation Project) wave spectrum was assumed to represent the average wave conditions over time; this gives the following spectral ratio between Te and Mwp: $Mwp < 6$ s 1.055, $Mwp < 10$ s 1.11, $Mwp > 10$ s 1.14 [54].

Stopa and Cheung [60] found the ERA-Interim to generally underestimate wave height; however, its performance very constant with similar errors through time. A small underestimation of wave height in the ERA-Interim data is also found by [61]. Other studies have also found underestimation of high wave heights, whilst on some occasions low wave heights have been underestimated [62,63].

Wave buoy data was made available by the Met Office for their K5 and K7 buoys (from 01/01/2010 00:00 to 01/07/2013 00:00) and the HebMarine project's wave buoys off the Isle of Lewis. The data from these buoys was compared to the modelled data from the ECMWF, with the results showing generally larger wave heights and shorter energy periods for measured data. These findings are generally in keeping with an extensive validation study carried out by the ECMWF [55] which shows small under predictions in wave heights (with a running 3 month model median falling between 0 m and -0.3 m of the measured median); these under predictions increase during winter months when wave heights are generally larger. Dee et al. [55] also examine wave period and find a degree of model bias. To account for these biases the following adjustments were made to the ERA-Interim data, based upon its relationship with the available wave buoy data (i.e. the Met Office K5 and K7 buoys and the HebMarine Bragar, Roag and Siadar buoys; further details are available in [64]).

$$Hs_b = Hs_a \times 1.1162 - 0.0849 \quad (3)$$

$$Te_b = Te_a \times 0.9186 + 0.2555 \quad (4)$$

where Hs_b is the adjusted Hs value and Hs_a is the unadjusted ECMWF Hs and Te_b is the adjusted Te value and Te_a is the unadjusted ECMWF Te.

The six hourly time steps of wave power is coarser, than that for wind generation. To align time steps to one hour wave data was linearly interpolated. Prior to this adjustment output was hindcast for wave power, using the methodology described in Section 2.3.3. The correlation between adjacent six hour time steps was compared for the adjusted wave parameters (Te and Hs) and hindcast generation. It was found the relationship in both instances was strong (generation R^2 0.825, Hs R^2 0.905, Te R^2 0.867, in all instances $p < 0.0001$),

however, the stronger relationships for Te and Hs means it is more appropriate to interpolate these values than output. A simple linear interpolation of the Te and Hs was carried out in order to create uniform one hour time steps for each of the three resources hindcast.

2.3.4. Calculating wave generation

To determine generation in this study power matrices were used for what were, in 2013, the two most prominent wave devices in Scotland, Pelamis and Oyster. These technologies were, in 2013, designated to the vast majority of the Crown Estate wave leases. How these were assigned in this study is displayed in Table 3. It should be noted that at the end of 2014 Pelamis filed for bankruptcy and Aquamarine (the developer of Oyster) laid off a large portion of their staff. However, even if different companies end up supplying alternative devices it is likely that the performance of these devices will be similar to Oyster and Pelamis.

The power matrices for these technologies [65] were applied to the adjusted ERA-Interim Te and Hs parameters. For both Pelamis and Oyster devices an array loss from device interaction of 10% is assumed, in line with the findings of [66]. An additional electrical loss of 3% is then applied, as used by [53].

2.4. NAO data

The NAO data used in this study comes from [67]. The dataset provides both monthly and seasonal NAO index values both of which are used in this study. The NAO index values are based on the difference of normalised sea level pressure between Lisbon (Portugal) and Stykkisholmur/Reykjavik (Iceland) [67].

2.5. Analysis approach

The analysis is split into three main sections. The first is an examination of the overall relationship between the NAO and renewable generation on both a monthly and seasonal scale. In addition to examining correlation between the NAO and generation a robust linear

Table 3

Areas leased by the Crown Estate for commercial wave farms. The West Orkney Middle South lease had no technology assigned but is abutted by two sites where Pelamis was the technology of choice, consequently Pelamis was the assumed technology at this lease.

Site name	Leased capacity (MW)	Likely device
Brough Head	200	Oyster
Costa Head	200	Oyster
Farr Point	50	Pelamis
Marwick Head	50	Pelamis
West Orkney Middle South	50	Undecided (Pelamis)
West Orkney South	50	Pelamis
Bernera	10	Pelamis
Galson	10	Oyster
North West Lewis	30	Oyster
South West Shetland	10	Pelamis

regression model is used to quantify the magnitude of the linear association between the NAO and electricity generation. The use of robust methods is considered to be effective in wind related applications by [68] due to their effectiveness in samples containing outliers. To help frame these findings of this model analysis of some of the economic implications is carried out.

The relationship between the NAO and short-term variability (i.e. daily and sub daily) is analysed to provide context from a system operation perspective – as the impact of short term variability on factors like reserve capacity can be substantial. Sinden [27] examines variability by calculating the change in power output and uses the standard deviations of these changes to measure variability. The same method is utilised within this study in Section 3.2.

The final major analysis element examines the shutdown of generating devices due to high-energy conditions. The occurrence of shutdowns caused by high-energy events throughout the year is explored, as is the association with these events with changes in the NAO. Additionally, the lost generation associated with these is examined in the context of winter NAO index values.

3. Results and analysis

In total output from 7755 MW of offshore wind, 5779 MW of onshore wind and 660 MW of wave developments was hindcast, making a combined 14194 MW. The NAO index was compared to generation for each resource individually and for the three of them combined for each month of the year; the results are displayed in Table 4.

The NAO index is shown to have a strong significant relationship for what can be considered as the higher energy - higher capacity factor – portion of the year, October through to March. This is also the half of the year when Scotland, and the UK as a whole, have the highest levels of electricity demand.

The NAO is often examined in the context of an overall winter index (taken as December, January, February and March) [67]; the relationship of this winter index with generation is presented in Fig. 3.

All analyses displayed in Fig. 3 e-h were carried out in R using RStudio [69,70]. The strength and significance of relationships between NAO and capacity factor were explored using Kendall's tau, as suggested for such applications by [71]. Linear trends were quantified using robust linear regression. The significance of robust linear model coefficient estimates were assessed by constructing 95% confidence intervals from standard errors.

In all months there is a positive correlation between the NAO and renewable generation (see Table 4). The strength of this correlation and its statistical significance increases during the higher energy half of the year (October to March). These fluctuating levels of generation caused by the NAO will impact income and payback rates for renewable developers and should be considered in risk models, particularly as recent

research suggests substantial increase in variability of the winter NAO [17]. This has implications for Scotland's energy system, as low NAO winters can be associated with extended periods of unusually low temperatures, which can increase energy demand.

Of the three renewable resources, the relationship between NAO and onshore wind is the most strongly positive (as expressed by a Kendall's tau 0.70). Further exploring this relationship, the linear association between NAO and onshore wind capacity factor is considerable; whereby the model (displayed in Fig. 3e) estimates an increase in NAO index of 1 equating to an increase in capacity factor of 2.59 (95% CI; 2.09, 3.08), which is 5.7% of the average winter capacity factor for onshore wind. In terms of offshore wind, the positive correlation with NAO is weaker than that for onshore wind (as expressed by a lower Kendall's tau of 0.56) and this is reflected by the larger confidence interval calculated for the robust regression slope coefficient (95% CI; 2.13, 4.20). Nevertheless, the associations between NAO and capacity factor for both onshore and offshore wind are comparable in magnitude. The strength of positive association between capacity factor for wave resource and NAO is similar to that of onshore wind (Kendall's tau 0.64) and this is reflected by the narrowest robust regression slope coefficient confidence interval (95% CI, 0.984, 1.71). However, perhaps owing to the relatively small range of capacity factors for wave power regardless of NAO (~40 to 53), the magnitude of the association between NAO and wave capacity factor is markedly lower than for either wind resource. Here, an increase in NAO of 1 equates to an increase in wave capacity factor of just 1.35; (95% CI; 0.984, 1.71), which equates to just 2.2% of average winter wave capacity factor. A possible influential factor in this smaller increase in capacity factor for wave power may relate to the relatively greater tendency for wave device shutdowns under higher NAO conditions than occur for wind turbines; this is explored in Section 3.3.

3.1. Economic implications

Associated with the impact of the NAO on renewable capacity factors is variability of income. A simple analysis of how the models displayed in Fig. 3e-h translate to income is provided in Table 5.

As wave power is the least mature technology it receives the greatest level of support, receiving a strike price under the CfD mechanism nearly three times that of offshore wind. However, this increased strike price means changes in NAO have the greatest impact per MW on income for wave power, despite the magnitude of the association between NAO and wave capacity factor being lower than for either wind resource. Given the immature nature of the technology, it is especially important for developers to take into account this potentially large variability in income in risk modelling.

The changes in income associated with NAO will also have implications for the onshore and offshore wind industry. This is useful to

Table 4

Correlation (Pearson's) between monthly NAO index values and renewable generation from the 30 year hindcast.

Month	Onshore wind		Offshore wind		Wave		Combined generation	
	r (p-value)	Capacity factor	r (p-value)	Capacity factor	r (p-value)	Capacity factor	r (p-value)	Capacity factor
Jan	0.737 (< 0.001)	39.1	0.622 (< 0.001)	64.7	0.538 (0.002)	46.8	0.678 (< 0.001)	52.1
Feb	0.828 (< 0.001)	38.4	0.822 (< 0.001)	61.0	0.830 (< 0.001)	46.0	0.838 (< 0.001)	50.0
Mar	0.763 (< 0.001)	37.9	0.617 (< 0.001)	58.0	0.638 (< 0.001)	44.7	0.685 (< 0.001)	48.3
Apr	0.408 (0.025)	30.2	0.501 (0.005)	43.0	0.325 (0.080)	34.8	0.479 (0.074)	37.1
May	0.310 (0.095)	26.4	0.318 (0.087)	35.1	0.388 (0.034)	23.7	0.327 (0.078)	31.0
Jun	0.345 (0.062)	23.8	0.400 (0.029)	33.1	0.568 (0.001)	19.8	0.413 (0.023)	28.7
Jul	0.301 (0.105)	21.1	0.231 (0.220)	30.3	0.230 (0.222)	16.7	0.255 (0.175)	26.1
Aug	0.449 (0.013)	21.7	0.119 (0.532)	35.1	0.482 (0.007)	20.4	0.233 (0.216)	29.0
Sep	0.410 (0.024)	27.3	0.311 (0.094)	44.8	0.443 (0.014)	32.4	0.363 (0.049)	36.8
Oct	0.582 (0.001)	31.8	0.554 (0.002)	55.6	0.608 (< 0.001)	42.2	0.589 (0.001)	44.5
Nov	0.574 (0.001)	33.0	0.560 (0.001)	60.0	0.453 (0.012)	45.1	0.586 (0.001)	47.3
Dec	0.818 (< 0.001)	32.5	0.791 (< 0.001)	58.7	0.715 (< 0.001)	45.3	0.817 (< 0.001)	46.4

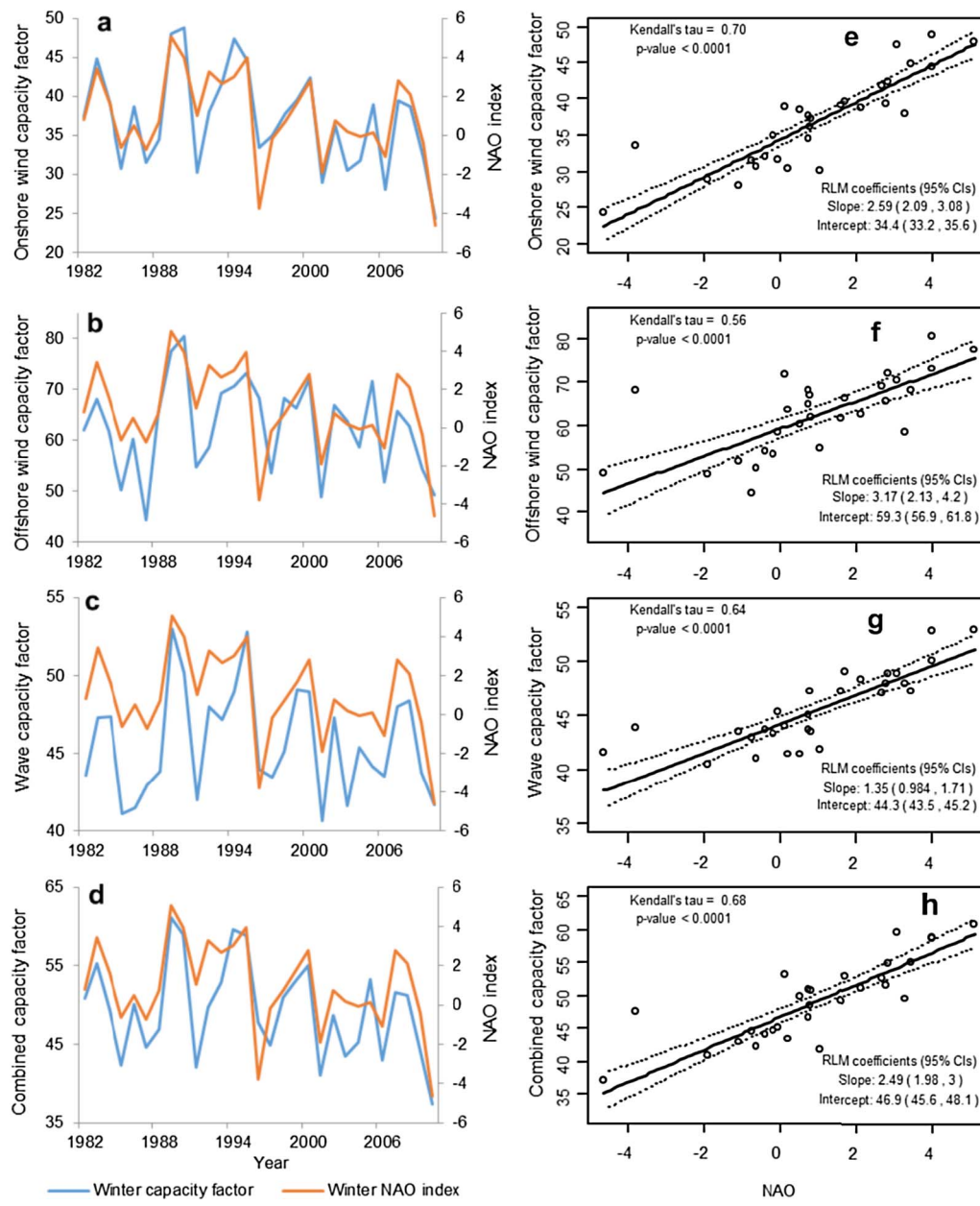


Fig. 3. Comparison of the hindcast winter capacity factor and the winter NAO index. In this case winter is taken to be December of the previous year with January, February and March of the year listed; from the 30 years of data this creates 29 winter periods. Figures a-d renewable generation and NAO index across the hindcast time series. Figures e-h analyses of the relationship between NAO index and hindcast capacity factors. Kendall's tau (similar to Spearman's rho) is a measure of monotonic/ordinal correlation between two variables (here NAO and capacity factor).

Table 5

Summary of winter income for the three different renewable resources in this study and the impact the NAO has on this. For onshore wind the average strike prices from the most recent UK Contracts for Difference (CfD) bidding round [72] is applied and for offshore wind and wave the 2021/22 CfD strike price agreed by the UK Government is used [73]. Generating capacity is accounted for (i.e. 7755 MW offshore wind, 5779 MW onshore wind, 660 MW wave) unless otherwise stated and a non-leap year is assumed. The differences in income are calculated from the impact of the NAO on capacity modelled in Fig. 3e-g with the equivalent slope coefficient confidence intervals provided in brackets.

	Onshore wind	Offshore wind	Wave
Strike price (£/MWh)	81.9	105.0	310.0
Theoretical maximum winter income (£ million)	1375.3	2364.7	594.2
Average winter capacity factor income (£ million)	508.0	1483.1	271.4
Difference in income for an increase in NAO index of 1 (£ million)	35.6 (28.7, 42.4)	75.0 (50.4, 99.3)	8.0 (5.8, 10.2)
Difference in income per MW for increase in NAO index of 1 (£ thousand)	6 (5.0, 7.3)	10 (6.5, 12.8)	12 (8.9, 15.4)

examine in the context of installed capacity price, which when taking the mean figures from the International Energy Agency, is 1233 and 3190 £/kW for onshore and offshore wind respectively [74]. Consequently, the modelled impacts of a change in the NAO index of 1 in a winter is the equivalent $\sim 1/200$ of the price of an onshore wind farm or $\sim 1/330$ of an offshore wind farm. If strongly negative NAO phases, such as the 2010 winter noted by [15], were to become more prevalent this could start to have a noticeable impact on payback rates over a project's lifetime.

3.2. Impact of NAO on variability

When examining long-term output trends, and their implications for the energy system, quantification of the variability is useful in understanding the characteristics of the resource. Sinden [27] examines variability by analysing the change in power output through the hindcast chronology. Sinden [27] calculates the change in power over both a 1 h and 4 h timestep, and the standard deviation of the resulting data series is calculated (expressed as a percentage of installed

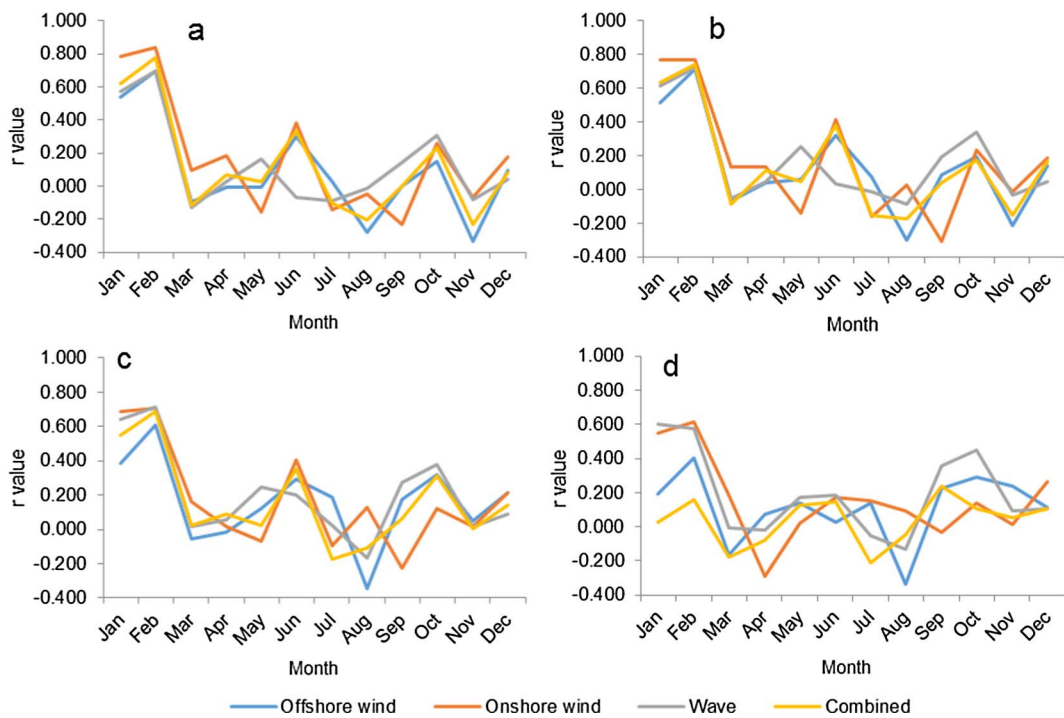


Fig. 4. Pearson's correlation analysis between 1, 4, 12 and 24 h ahead variability in output and monthly NAO index values. For 0.01 level of significance $r = 0.463$. (a) 1 h ahead variability. (b) 4 h ahead variability. c. 12 h ahead variability. d. 24 h ahead variability.

capacity). In this analysis the 1 and 4 h timesteps are kept and additional 12 and 24 h timesteps are added to give a longer viewpoint (a 24 h timestep is useful to include as it puts the analysis in the context of the day ahead electricity market). The standard deviations at these time intervals were calculated for each of the 360 months in the hindcast, with Pearson's correlation analysis being undertaken between these and the corresponding monthly NAO index values. The results of these are summarised in Fig. 4.

Only the two highest generation months, January and February, have statistically significant relationships between the monthly NAO and variability in generation, with a positive correlation being displayed. So whilst high NAO Januaries and Februaries result in greater levels of generation they are also associated with greater variability. From an electricity system management perspective, this means this more changeable generation needs to be controlled, through a combination of advanced forecasting and system management solutions such as storage and export. Alternatively, if renewables have priority dispatch these issues are no longer present; however, the electricity system will need greater flexibility in terms of ramp up and higher levels of reserve capacity.

For variability on the shorter timescales (1 and 4 h ahead periods) statistically significant relationships between the monthly NAO index and generation variability for January and February are observed for all four portfolios – onshore wind, offshore wind, wave and the combined resources. Whilst for the 12 and 24 h ahead periods this relationship is only statistically significant for onshore wind and wave power. At the 24 h ahead variability in particular Fig. 4 shows the value of renewable resource diversity as the combined resources exhibit very little increased variability over this period, even in the high energy winter months. Illustrating the importance of considering resource diversity in renewable integration planning.

3.3. Increased shutdowns in positive NAO conditions

In general, the results presented in Table 4 show the highest energy months display the strongest correlation with the NAO. However, there is a markedly lower r and higher p -value for wave power in January

than for other winter months (December, February and March). Neill et al. [75] show that January is the month associated with the highest wave energy in Scotland. However, highest wave energy does not necessarily mean highest generation from devices, as in very high-energy events devices have too shutdown. To explore whether this was a likely reason behind the lower correlation between the NAO index and generation in January, an assessment of shutdowns due to high-energy events was undertaken. The power matrices used have devices entering 'survival' mode (i.e. they cease generate) in seas with H_s over 3 m if wave frequencies are high (i.e. $T_e < 5$ s); as waves get larger devices enter 'survival' mode in lower frequency conditions (e.g. for Pelamis with an H_s of 5 m devices will enter 'survival' mode with $T_e < 6.5$ s) [65]. Consequently, H_s being greater than 3 m but no output being hindcast is a measure of times when there is no generation due to devices entering 'survival' mode. The number of occurrences that wave heights were greater than 3 m but zero generation was hindcast was calculated as a mean value for the wave portfolio for each of the 360 hindcast months. These were then transformed into percentage of time figures; the results are displayed for each month of the year in Fig. 5.

As would be expected, given it is the highest energy month, January experiences the highest proportion of time when devices are in survival mode. Pearson's analysis was carried out on monthly NAO index values and the average percentage of time devices are in survival mode. This relationship is statistically significant (p values < 0.01) for the months in the winter half of the year: January $r = 0.657$ ($p < 0.001$), February $r = 0.630$ ($p < 0.001$), March $r = 0.628$ ($p < 0.001$), October $r = 0.240$ ($p = 0.003$), November $r = 0.519$ ($p < 0.001$) and December $r = 0.522$ ($p < 0.001$). So despite these months having the highest energy available [75] the additional energy associated with positive NAO conditions may not be able to be effectively exploited with current wave technology.

Similarly, to wave power, in Table 4, January offshore wind generation shows a lower correlation between generation and the NAO index than December and February. Instances when wind speeds exceed the minimum that is needed for maximum generation were examined, with the occasions that generation was below full capacity despite these

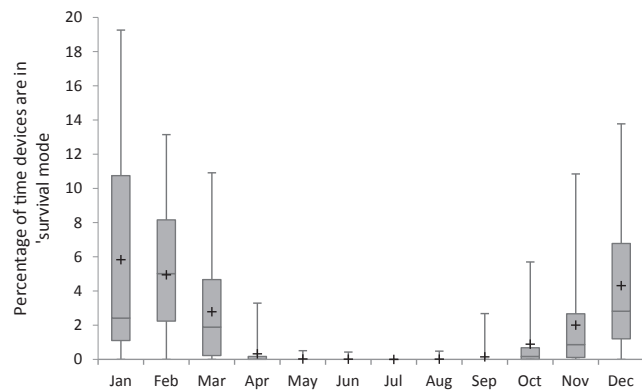


Fig. 5. The time high energy sea conditions result in wave farms switching to 'survival' mode. The data used are the mean of the 10 wave leases for each of the 360 months in the hindcast. The error bars represent the maximum and minimum percentage of time devices are in 'survival' mode over the 30 year chronology; the boxes mark the interquartile range, the line across them the median and the + marks the mean.

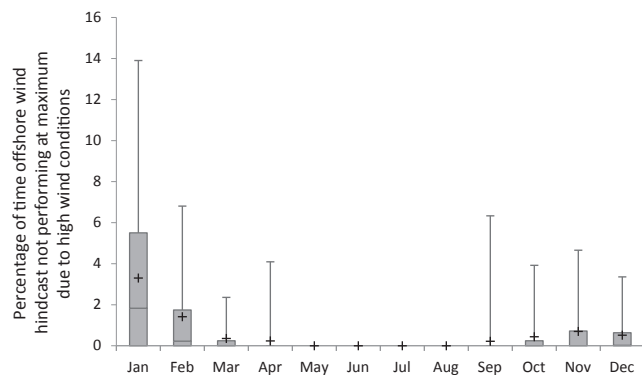


Fig. 6. Percentage of time hindcast offshore wind farm areas are not performing at maximum output due to high wind speed conditions. The error bars represent the maximum and minimum percentage of time devices are in 'survival' mode over the 30 year chronology; the boxes mark the interquartile range, the line across them the median and the + marks the mean.

high wind speeds being counted (i.e. conditions where some turbines are cutting out due to high wind speeds); the results are displayed in Fig. 6. This differs from the methodology used to create Fig. 5 where there is total shutdown of devices in a renewable farm, whereas in Fig. 6 some turbines are still operating in most instances.

Unlike Fig. 5, where the percentage time is for zero generation from wave power, Fig. 6 includes times where electricity is still being generated. Therefore, the higher percentages of time in Fig. 5 are even more marked. Thus whilst higher wind speeds, such as those associated with higher NAO values, do cause some reduction in offshore generation due to shutdowns the impact of this is far lower for offshore wind than wave power. This is likely due to technology maturity and the associated differences in how wave and offshore wind farms function in high-energy conditions. For example, at the Islay offshore wind site there were only 120 h in the 30 year hindcast where there was no generation due to high wind conditions; whilst at the North West Lewis wave site there were 3307 h during the 30 years when devices did not generate due to high-energy sea conditions.

The impact of high-energy conditions associated with the NAO is explored further in the context of generation in Fig. 7. This Figure displays the generation lost due to wave devices entering survival mode and offshore wind farms generating at reduced levels due to high wind speed conditions in each of the 29 full NAO winters in the hindcast (December to March) and the corresponding winter NAO index.

The n of two for the < -2 winter NAO index bin in Figure is too small to draw information from, however, when examining the other

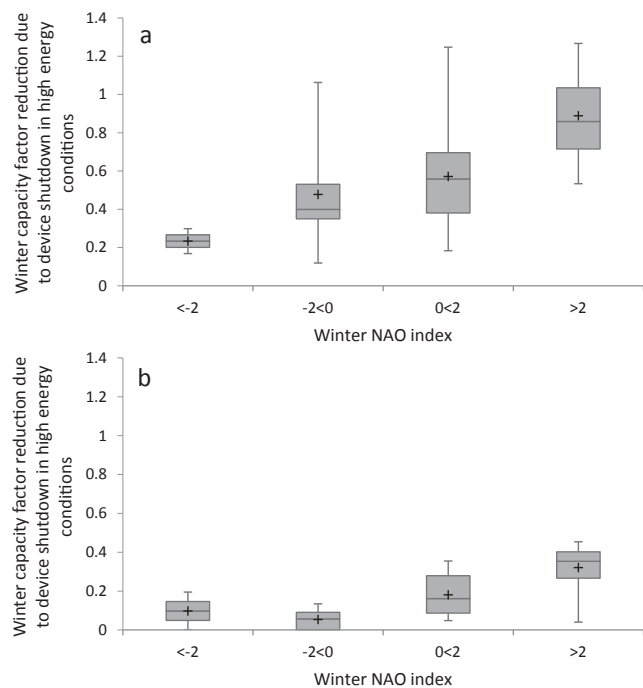


Fig. 7. Electricity not generated in winter due to high-energy conditions as a percentage of theoretical maximum winter generation plotted against the corresponding winter NAO index bin. Figure a wave power and Figure b offshore wind. Bin $< -2n = 2$, $-2 < 0n = 7$, $0 < 2n = 10$, $> 2n = 10$. The error bars represent the maximum and minimum percentage of time devices are in 'survival' mode over the 30 year chronology; the boxes mark the interquartile range, the line across them the median and the + marks the mean.

three bins it is clear that with increasingly positive winter NAO index values comes an increasing loss in capacity factor due to device shutdown in high energy conditions. Fig. 7 also illustrates a much larger associated loss for wave power than offshore wind.

From a system management perspective there is a danger of decreased offshore wind generation – due to high wind conditions – being associated with wave devices entering survival mode, as this would require challenging fast backup capacities. This was investigated and 47% of the instances when offshore wind generation was reduced due to high wind speed conditions were associated with at least one of the wave farms modelled entering survival mode. However, this accounts for 0.2% of the 30 year hindcast, whilst at least one of the modelled wave areas was in survival mode for 3.7% of the hindcast; compared to at least one offshore wind farm not functioning at full capacity due to high winds for 0.4% of the time. Related to this the impact on capacity factor reduction is far higher for wave than offshore wind; for example, in strongly positive winters (NAO index > 2) wave device shutdowns reduce the mean winter capacity factor by 0.89 for wave power compared to 0.32 for offshore wind (see Fig. 7). Consequently, wave devices entering survival mode would become the largest concern for potential electricity shortfall due to high-energy NAO conditions if the capacity expands to multi GW levels, as this study suggests it is associated with ~ 3 times the reduction in capacity factor compared to offshore wind. However, given the far greater level of offshore wind capacity considered in this study (11.75 times that of wave) at the current time it is the losses associated with this resource which will have more impact on overall portfolio performance.

For onshore wind generation the large number of wind farms within one modelling area and the influences of local topography and roughness makes the impact of extreme conditions on generation hard to accurately breakdown quantitatively. As with wave power and offshore wind January shows a lower correlation between generation and the NAO index in Table 4 than December and February; however, this

difference is not as large.

3.3.1. Discussion of ecological impacts associated with high-energy events

Another consideration is that the NAO is responsible for much of the inter-annual variation in seawater temperature. In north-western Europe this relationship is particularly closely linked with positive phases of NAO resulting in periods of warmer seawater during the winter and persisting through the spring [11]. This increased seawater temperature has been shown to result in changes to the composition of encrusting biological communities [76–78] increased recruitment [79] and a lengthened growing season for marine organisms [80] such as kelp, barnacles and mussels. Following periods of positive NAO index values, we therefore see increased growth of marine species such as these, collectively termed biofouling, on man-made structures [81] such as wave energy devices. Increased biofouling can have a negative effect on the efficiency of wave energy extraction devices [82–85] due to increased drag and inertia loads [86,87]. It can also lead to increased chances of device failure due to accelerated corrosion [88,89] and the added mass which leads to increased wear and fatigue-loading of components [90]. A knock-on impact of a high NAO winter for wave power may therefore be that, despite the potential increase in generation over the winter, the efficiency of wave energy extraction maybe reduced by increased biofouling during the subsequent spring and summer.

4. Discussion of mitigating the impact of the NAO on renewable generation

Hanna et al. [17] observe a “striking” increase in variability of the winter NAO in recent years. This increased variability, coupled with increased renewable penetration, makes mitigation of the low generation in Scotland associated with negative NAO important to consider. Seemingly, one of the most effective ways to do this is greater European scale grid integration. Jerez et al. [91] performed a similar study to this one for Spain and Portugal, showing in this area of Europe negative NAO phases enhances wind speeds at turbine hub height by ~30% and also increases precipitation and associated hydropower generation. A further study examining several regions across Europe also shows areas which would be complementary to the output modelled in this study, with solar PV in Germany and Belarus performing better in negative NAO phases than positive ones and once again onshore wind in Spain (Andalucía) [92]. The complimentary nature of the impact of the NAO on renewable resources across Europe is potentially an important variability management tool and merits in depth exploration in future studies. Greater understanding of this could result in the assignment of additional value to trans-European super-grid projects, making them more attractive to policy makers. This is important to consider given the high economic costs associated with such projects.

A recent study [16] develops a new climate index, West Europe Pressure Anomaly (WEPA). It is based on the sea level pressure gradient between Valencia (Ireland) and Santa Cruz de Tenerife (Canary Islands) and is strongly related to extreme winter events. In particular, the winter 2013/2014, categorised as one the most impactful on European Atlantic coast of the past 70 years, the accuracy of WEPA is supported [93]. WEPA controls storm variability for up to 90% of European Atlantic coast observed winter-averaged Hs southward of 52° [16]. Despite the NAO not being exceptional during the 2013/2014 storm event, it has a huge impact on Scotland and Ireland west coast, controlling more than 86% of winter-averaged Hs variability in these areas [16]. How the forcing of WEPA in more southerly latitudes and the NAO in northerly latitudes interact in terms of renewable output is likely to be an important avenue of further research in this area.

5. Conclusion

There is a strongly significant relationship between wave, onshore

wind and offshore wind generation and the NAO for the whole winter half of the year (October–March). In general, the highest correlations between generation and NAO index are observed for onshore wind; given that this is currently the largest renewable in terms of installed capacity in Scotland this is important to recognise for electricity system management. However, the NAO had the strongest influence on capacity factor for offshore wind, with each increase in NAO index of 1 causing a predicted increase of capacity factor of 3.17 (compared to 2.59 for onshore wind, 1.35 for wave, and 2.49 for the combined portfolio). Offshore wind is set to make up an increasingly large portion of Scotland's generating capacity, with several large projects modelled in this study progressing in development. The variability in generation in winter months caused by the NAO should therefore be considered in regard to security of supply, particularly in the context of high demand low NAO winters.

The higher energy associated with a positive NAO index is not always exploitable. In the case of wave power there is a statistically significant positive correlation between NAO index and increased generating device shutdown for the six highest energy months of the year (October through to March). This is also reflected in generation, for example in highly positive NAO conditions (winter NAO index > 2) there is a mean reduction in capacity factor of 0.89 due to device shutdown.

The NAO also exhibited a positive correlation with variability in generation. This is statistically significant in January and February for all three resources and the combined portfolio at 1 and 4 h ahead time scale but at the 12 and 24 h ahead level only for onshore wind and wave generation. Increased variability tends to make integration and utilisation of renewables harder, so although high NAO years are likely to bring increased generation they will also present some management challenges. These and other challenges posed by the influence of the NAO on renewable generation would in part be mitigated by greater European scale electricity integration. This would enable the differing influences of climate teleconnections in different geographic areas on renewable generation to be exploited, potentially enhancing energy security.

Acknowledgements

The authors acknowledge the support of Highlands and Islands Enterprise, the Scottish Funding Council and the European Regional Development Fund (ERDF) through the Supergen Plus program. We also wish to thank and acknowledge Arne Vögler (Hebridean Marine Energy Futures) and the Met Office for wave buoy data provision. Thanks are also due to Kenny Boyd for his data presentation suggestions and Joss Ratcliffe for note taking and minuting meetings. The authors are also grateful to Emily Kearn, Diego Del Villar and Róisín Kelliher for their help and support. Finally, we would like to thank the reviewers of this manuscript for their time and suggestions – their input was helpful and appreciated.

References

- [1] The Scottish Government. 2020 Routemap for Renewable Energy in Scotland 2011. <http://www.scotland.gov.uk/Resource/Doc/917/0118802.pdf> (accessed December 6, 2012).
- [2] DECC. Digest of United Kingdom Energy Statistics. Off Natl Stat 2015. https://www.gov.uk/government/uploads/system/uploads/attachment_data/file/450302/DUKES_2015.pdf (accessed March 18, 2016).
- [3] Barnston AG, Livezey RE. Classification, seasonality and persistence of low-frequency atmospheric circulation patterns. Mon Weather Rev 1987;115:1083–126. [http://dx.doi.org/10.1175/1520-0493\(1987\)115<1083:CSAPOL>2.0.CO;2](http://dx.doi.org/10.1175/1520-0493(1987)115<1083:CSAPOL>2.0.CO;2).
- [4] Miettinen A, Koç N, Hall IR, Godtliebsen F, Divine D. North Atlantic sea surface temperatures and their relation to the North Atlantic Oscillation during the last 230 years. Clim Dyn 2011;36:533–43. <http://dx.doi.org/10.1007/s00382-010-0791-5>.
- [5] Marshall J, Kushnir Y, Battisti D, Chang P, Czaja A, Dickson R, et al. North Atlantic climate variability: phenomena, impacts and mechanisms. Int J Climatol 2001;21:1863–98. <http://dx.doi.org/10.1002/joc.693>.
- [6] Hurrell JW, van Loon H. Decadal variations in climate associated with the north

atlantic oscillation. *Clim Change* 1997;36:301–26. <http://dx.doi.org/10.1023/A:1005314315270>.

[7] Trigo R, Osborn T, Corte-Real J. The North Atlantic Oscillation influence on Europe: climate impacts and associated physical mechanisms. *Clim Res* 2002;20:9–17. <http://dx.doi.org/10.3354/cr020009>.

[8] Curry RG, McCartney MS. Ocean gyre circulation changes associated with the north atlantic oscillation*. *J Phys Oceanogr* 2001;31:3374–400. [http://dx.doi.org/10.1175/1520-0485\(2001\)031<3374:OGCAW>2.0.CO;2](http://dx.doi.org/10.1175/1520-0485(2001)031<3374:OGCAW>2.0.CO;2).

[9] Fratantoni DM. North Atlantic surface circulation during the 1990's observed with satellite-tracked drifters. *J Geophys Res Ocean* 2001;106:22067–93. <http://dx.doi.org/10.1029/2000JC000730>.

[10] Cayan DR. Latent and sensible heat flux anomalies over the northern oceans: driving the sea surface temperature. *J Phys Oceanogr* 1992;22:859–81. [http://dx.doi.org/10.1175/1520-0485\(1992\)022<0859:LASHFA>2.0.CO;2](http://dx.doi.org/10.1175/1520-0485(1992)022<0859:LASHFA>2.0.CO;2).

[11] Hurrell JW. Decadal trends in the north atlantic oscillation: regional temperatures and precipitation. *Science* 1995;269(80):676–9. <http://dx.doi.org/10.1126/science.269.5224.676>.

[12] Osborn T. North Atlantic Oscillation. *Clim Res Unit: Univ East Angl*; 2000 <http://www.cru.uea.ac.uk/documents/421974/1295957/Info+sheet+#+11.pdf/bc0835c5-d31-4b70-be72-1a7035e59b6e1> (accessed July 18, 2014).

[13] Curtis J, Lynch MÁ, Zubiate L. Carbon dioxide (CO₂) emissions from electricity: the influence of the North Atlantic Oscillation. *Appl Energy* 2016;161:487–96. <http://dx.doi.org/10.1016/j.apenergy.2015.09.056>.

[14] Earl N, Dorling S, Hewston R, von Glasow R. 1980–2010 variability in U.K. surface wind climate. *J Clim* 2013;26:1172–91. <http://dx.doi.org/10.1175/JCLI-D-12-00026.1>.

[15] Ely CR, Brayshaw DJ, Methven J, Cox J, Pearce O. Implications of the North Atlantic Oscillation for a UK–norway renewable power system. *Energy Policy* 2013;62:1420–7. <http://dx.doi.org/10.1016/j.enpol.2013.06.037>.

[16] Castelle B, Dodet G, Masselink G, Scott T. A new climate index controlling winter wave activity along the Atlantic coast of Europe: the West Europe Pressure Anomaly. *Geophys Res Lett* 2017;44:1384–92. <http://dx.doi.org/10.1002/2016GL072379>.

[17] Hanna E, Cropper TE, Jones PD, Scaife AA, Allan R. Recent seasonal asymmetric changes in the NAO (a marked summer decline and increased winter variability) and associated changes in the AO and Greenland Blocking Index. *Int J Climatol* 2015;35:2540–54. <http://dx.doi.org/10.1002/joc.4157>.

[18] Kriesche P, Schlosser CA. The association of the north atlantic and the arctic oscillation on wind energy resource over europe and its intermittency. *Energy Procedia* 2014;59:270–7. <http://dx.doi.org/10.1016/j.egypro.2014.10.377>.

[19] Brayshaw DJ, Troccoli A, Fordham R, Methven J. The impact of large scale atmospheric circulation patterns on wind power generation and its potential predictability: a case study over the UK. *Renew Energy* 2011;36:2087–96. <http://dx.doi.org/10.1016/j.renene.2011.01.025>.

[20] Neill SP, Vögler A, Goward-Brown AJ, Baston S, Lewis MJ, Gillibrand PA, et al. The wave and tidal resource of Scotland. *Renew Energy* 2017. <http://dx.doi.org/10.1016/j.renene.2017.03.027>.

[21] Santo H, Taylor PH, Eatock Taylor R, Stansby P. Decadal variability of wave power production in the North-East Atlantic and North Sea for the M4 machine. *Renew Energy* 2016;91:442–50. <http://dx.doi.org/10.1016/j.renene.2016.01.086>.

[22] Dodet G, Bertin X, Taborida R. Wave climate variability in the North-East Atlantic Ocean over the last six decades. *Ocean Model* 2010;31:120–31. <http://dx.doi.org/10.1016/j.ocemod.2009.10.010>.

[23] Cradden LC, McDermott F, Zubiate L, Sweeney C, O'Malley M. A 34-year simulation of wind generation potential for Ireland and the impact of large-scale atmospheric pressure patterns. *Renew Energy* 2017;106:165–76. <http://dx.doi.org/10.1016/j.renene.2016.12.079>.

[24] Curtis J, Lynch MÁ, Zubiate L. The impact of the North Atlantic Oscillation on electricity markets: a case study on Ireland. *Energy Econ* 2016;58:186–98. <http://dx.doi.org/10.1016/j.eneco.2016.07.003>.

[25] Arguez A, Vose RS. The definition of the standard WMO climate normal: the key to deriving alternative climate normals. *Bull Am Meteorol Soc* 2011;92:699–704. <http://dx.doi.org/10.1175/2010BAMS2955.1>.

[26] Früh W-G. Long-term wind resource and uncertainty estimation using wind records from Scotland as example. *Renew Energy* 2013;50:1014–26. <http://dx.doi.org/10.1016/j.renene.2012.08.047>.

[27] Sinden G. Characteristics of the UK wind resource: Long-term patterns and relationship to electricity demand. *Energy Policy* 2007;35:112–27. <http://dx.doi.org/10.1016/j.enpol.2005.10.003>.

[28] Boehme T, Wallace A. Hindcasting hourly wind power across scotland based on met station data. *Wind Energy* 2008;11:233–44. <http://dx.doi.org/10.1002/we.257>.

[29] Sharp E, Dodds P, Barrett M, Spataru C. Evaluating the accuracy of CFSR reanalysis hourly wind speed forecasts for the UK, using in situ measurements and geographical information. *Renew Energy* 2015;77:527–38. <http://dx.doi.org/10.1016/j.renene.2014.12.025>.

[30] Dragoon K. Developing Useful Wind Generation Data. Valuing Wind Gener. Integr. Power Syst. Elsevier; 2010. p. 37. <http://dx.doi.org/10.1016/B978-0-8155-2047-4.10004-3>.

[31] BADC. Met Office - MIDAS Land Surface Stations data (1853-current) 2013. http://badc.nerc.ac.uk/view/badc.nerc.ac.uk_ATOM_dataent_ukmo-midas (accessed December 10, 2013).

[32] Boehme T, Taylor J, Wallace R, Bialek J. Matching renewable electricity generation with demand. scottish executive; 2006.

[33] Früh W-G. From local wind energy resource to national wind power production. *AIMS Energy* 2015;3:101–20. <http://dx.doi.org/10.3934/energy.2015.1.101>.

[34] Onat N, Ersoz S. Analysis of wind climate and wind energy potential of regions in Turkey. *Energy* 2011;36:148–56. <http://dx.doi.org/10.1016/j.energy.2010.10.059>.

[35] Mortensen NG, Petersen EL. Influence of topographical input data on the accuracy of wind flow modelling in complex terrain. *Eur Union Wind Energy Conf* 1997.

[36] European Environment Agency. Corine Land Cover 2006 raster data 2012. <http://www.eea.europa.eu/data-and-maps/data/corine-land-cover-2006-raster-2> (accessed February 6, 2013).

[37] Technical University of Denmark. Roughness Maps from Gridded Land Cover Information 2012. http://www.wasp.dk/Support/FAQ/GriddedRoughness.aspx?sc_lang=en.

[38] Nielsen TS, Joensen A, Madsen H, Landberg L, Giebel G. A new reference for wind power forecasting. *Wind Energy* 1998;1:29–34. [http://dx.doi.org/10.1002/\(SICI\)1099-1824\(199809\)1:1<29::AID-WE10>3.0.CO;2-B](http://dx.doi.org/10.1002/(SICI)1099-1824(199809)1:1<29::AID-WE10>3.0.CO;2-B).

[39] McKenna R, Hollnacher S, Fichtner W. Cost-potential curves for onshore wind energy: A high-resolution analysis for Germany. *Appl Energy* 2014;115:103–15. <http://dx.doi.org/10.1016/j.apenergy.2013.10.030>.

[40] Blanco MI. The economics of wind energy. *Renew Sustai Energy Rev* 2009;13:1372–82. <http://dx.doi.org/10.1016/j.rser.2008.09.004>.

[41] Ali M, Matevosyan J, Milanović JV. Probabilistic assessment of wind farm annual energy production. *Electr Power Syst Res* 2012;89:70–9. <http://dx.doi.org/10.1016/j.epdr.2012.01.019>.

[42] NASA. MERRA: Modern-Era retrospective analysis for research and applications 2014. <http://gmao.gsfc.nasa.gov/merra/> (accessed April 3, 2014).

[43] Rienerer MM, Suarez MJ, Gelaro R, Todling R, Bacmeister J, Liu E, et al. MERRA: NASA's Modern-Era retrospective analysis for research and applications. *J Clim* 2011;24:3624–48. <http://dx.doi.org/10.1175/JCLI-D-11-00015.1>.

[44] National Center for Atmospheric Research Staff (Eds). The Climate Data Guide: NASA MERRA 2014. <https://climatedataguide.ucar.edu/climate-data/nasa-merra> (accessed March 26, 2014).

[45] Crown Estate. UK MERRA Validation With Offshore Meteorological Data 2014. <http://www.thecrownestate.co.uk/media/389807/ei-uk-merra-validation-with-offshore-meteorological-data.pdf> (accessed June 23, 2015).

[46] Kiss P, Jánosi IM. Comprehensive empirical analysis of ERA-40 surface wind speed distribution over Europe. *Energy Convers Manag* 2008;49:2142–51. <http://dx.doi.org/10.1016/j.enconman.2008.02.003>.

[47] NCAR & UCAR. Wind direction quick reference. *Earth Obs Lab* 2017. <https://www.eol.ucar.edu/content/wind-direction-quick-reference> (accessed May 26, 2017).

[48] Crown Estate. Energy & Infrastructure: Maps and GIS Data 2013. <http://www.thecrownestate.co.uk/energy-infrastructure/downloads/maps-and-gis-data/> (accessed December 9, 2013).

[49] Pérez B, Mínguez R, Guanche R. Offshore wind farm layout optimization using mathematical programming techniques. *Renew Energy* 2013;53:389–99. <http://dx.doi.org/10.1016/j.renene.2012.12.007>.

[50] Fang H-F. Wind energy potential assessment for the offshore areas of Taiwan west coast and Penghu Archipelago. *Renew Energy* 2014;1–5. <http://dx.doi.org/10.1016/j.renene.2013.11.047>.

[51] Lange B, Hojstrup J. WASP for offshore sites in confined coastal waters: the influence of the sea fetch. *EWEC-CONFERENCE- 1999*.

[52] Lange B, Hojstrup J. Evaluation of the wind-resource estimation program WASP for offshore applications. *J Wind Eng Ind* ... 2001.

[53] Stoutenburg ED, Jenkins N, Jacobson MZ. Power output variations of co-located offshore wind turbines and wave energy converters in California. *Renew Energy* 2010;35:2781–91. <http://dx.doi.org/10.1016/j.renene.2010.04.033>.

[54] ABPmer. Atlas of UK Marine Renewable Energy Resources 2008. <http://www.renewables-atlas.info/> (accessed April 18, 2014).

[55] Dee DP, Uppala SM, Simmons AJ, Berrisford P, Poli P, Kobayashi S, et al. The ERA-Interim reanalysis: configuration and performance of the data assimilation system. *Q J R Meteorol Soc* 2011;137:553–97. <http://dx.doi.org/10.1002/qj.828>.

[56] ECMWF. ECMWF Wave Model 2008. <http://www.ecmwf.int/research/ifsdocs/CY33r1/WAVES/IFSPart7.pdf> (accessed July 3, 2013).

[57] ECMWF. The ocean wave model 2013. http://www.ecmwf.int/products/forecasts/guide/The_ocean_wave_model.html (accessed August 21, 2013).

[58] ECMWF. Global Wave Analysis Data Set 2013. <http://www.ecmwf.int/products/data/archive/descriptions/od/wave/an/g/index.html> (accessed June 27, 2013).

[59] Holthuijsen LH. Waves in Oceanic and Coastal Waters. Cambridge: Cambridge University Press; 2007.

[60] Stopa JE, Cheung KF. Intercomparison of wind and wave data from the ECMWF reanalysis Interim and the NCEP climate forecast system reanalysis. *Ocean Model* 2014;75:65–83. <http://dx.doi.org/10.1016/j.ocemod.2013.12.006>.

[61] van Nieuwkoop JCC, Smith HCM, Smith GH, Johannig L. Wave resource assessment along the Cornish coast (UK) from a 23-year hindcast dataset validated against buoy measurements. *Renew Energy* 2013;58:1–14. <http://dx.doi.org/10.1016/j.renene.2013.02.033>.

[62] Semedo A, Sušelj K, Rutgersson A, Sterl A. A global view on the wind sea and swell climate and variability from ERA-40. *J Clim* 2011;24:1461–79. <http://dx.doi.org/10.1175/2010JCLI3718.1>.

[63] Sterl A, Caires S. Climatology, variability and extrema of ocean waves: the Web-based KNMI/ERA-40 wave atlas. *Int J Climatol* 2005;25:963–77. <http://dx.doi.org/10.1002/joc.1175>.

[64] Commin AN. Matching renewable electricity supply to electricity demand in Scotland. University of Aberdeen; 2015.

[65] Silva D, Rusu E, Soares C. Evaluation of various technologies for wave energy conversion in the Portuguese Nearshore. *Energies* 2013;6:1344–64. <http://dx.doi.org/10.3390/en6031344>.

[66] Babarit A. On the park effect in arrays of oscillating wave energy converters. *Renew Energy* 2013;58:68–78. <http://dx.doi.org/10.1016/j.renene.2013.03.008>.

[67] Hurrell J, National Center for Atmospheric Research Staff (Eds). The Climate Data

Guide: Hurrell North Atlantic Oscillation (NAO) Index (station-based) 2013.

[68] Soukissian TH, Karathanasi FE. On the use of robust regression methods in wind speed assessment. *Renew Energy* 2016;99:1287–98. <http://dx.doi.org/10.1016/j.renene.2016.08.009>.

[69] RStudio Team. RStudio: Integrated Development for R 2015.

[70] R Core Team. R: A Language and Environment for Statistical Computing 2012.

[71] Della-Marta PM, Haylock MR, Luterbacher J, Wanner H. Doubled length of western European summer heat waves since 1880. *J Geophys Res* 2007;112:D15103. <http://dx.doi.org/10.1029/2007JD008510>.

[72] UK Government. Contracts for Difference (CFD) Allocation Round One Outcome 2015. https://www.gov.uk/government/uploads/system/uploads/attachment_data/file/407059/Contracts_for_Difference_-_Auction_Results_-_Official_Statistics.pdf (accessed June 3, 2017).

[73] UK Government. Contracts for Difference: An explanation of the methodology used to set administrative CFD strike prices for the next CFD allocation round 2016. https://www.gov.uk/government/uploads/system/uploads/attachment_data/file/566337/CONTRACT_FOR_DIFFERENCE_STRIKE_PRICE METHODOLOGY_final.pdf (accessed June 2, 2017).

[74] International Energy Agency. Projected Costs of Generating Electricity 2015. <https://www.iea.org/publications/freepublications/publication/ElecCost2015.pdf> (accessed June 3, 2017).

[75] Neill SP, Lewis MJ, Hashemi MR, Slater E, Lawrence J, Spall SA. Inter-annual and inter-seasonal variability of the Orkney wave power resource. *Appl Energy* 2014;132:339–48. <http://dx.doi.org/10.1016/j.apenergy.2014.07.023>.

[76] Hagberg J, Tunberg BG. Studies on the Covariation between Physical Factors and the Long-Term Variation of the Marine Soft Bottom Macrofauna in Western Sweden. *Estuar Coast Shelf Sci* 2000;50:373–85. <http://dx.doi.org/10.1006/ecss.1999.0578>.

[77] Birchenough SNR, Reiss H, Degraer S, Mieszkowska N, Borja Á, Buhl-Mortensen L, et al. Climate change and marine benthos: a review of existing research and future directions in the North Atlantic. *Wiley Interdiscip Rev Clim Chang* 2015;6:203–23. <http://dx.doi.org/10.1002/wcc.330>.

[78] Tunberg B, Nelson W. Do climatic oscillations influence cyclical patterns of soft bottom macrobenthic communities on the Swedish west coast? *Mar Ecol Prog Ser* 1998;170:85–94. <http://dx.doi.org/10.3354/meps170085>.

[79] Fisher AD, Petraitis PS. Large Spatial scale and long temporal-scale patterns of *Mytilus edulis* recruitment on rocky shores in Maine. *Benthic Ecol Meet, Mobile (Alabama): 2004*.

[80] Ottersen G, Planque B, Belgrano A, Post E, Reid P, Stenseth N. Ecological effects of the North Atlantic Oscillation. *Oecologia* 2001;128:1–14. <http://dx.doi.org/10.1007/s004420100655>.

[81] Osman R, Munguia P, Whittle R, Zajac R, Hamilton J. Thresholds and multiple community states in marine fouling communities: integrating natural history with management strategies. *Mar Ecol Prog Ser* 2010;413:277–89. <http://dx.doi.org/10.3354/meps08673>.

[82] Langhamer O, Haikonen K, Sundberg J. Wave power—Sustainable energy or environmentally costly? a review with special emphasis on linear wave energy converters. *Renew Sustain Energy Rev* 2010;14:1329–35. <http://dx.doi.org/10.1016/j.rser.2009.11.016>.

[83] Langhamer O, Wilhelmsson D, Engström J. Artificial reef effect and fouling impacts on offshore wave power foundations and buoys – a pilot study. *Estuar Coast Shelf Sci* 2009;82:426–32. <http://dx.doi.org/10.1016/j.ecss.2009.02.009>.

[84] von Jouanne A, Brekke T, Lettenmaier T, Amon E, Moran S, Yokochi A. Research and ocean testing solutions to advance the wave energy industry. 2014 IEEE PES Gen. Meet. | Conf. Expo. IEEE; 2014. p. 1–5. <http://dx.doi.org/10.1109/PESGM.2014.6939009>.

[85] Titah-Benbouzid H, Benbouzid M. Marine renewable energy converters and bio-fouling: A review on impacts and prevention. *EWTEC 2015, Nantes, France. Proc. 2015 EWTEC*, 2015.

[86] Yan T, Yan W, Dong Y, Wang H, Yan Y, Liang G. Marine fouling of offshore installations in the northern Beibu Gulf of China. *Int Biodeterior Biodegradation* 2006;58:99–105. <http://dx.doi.org/10.1016/j.ibiod.2006.07.007>.

[87] Jusoh I, Wolfram J. Effects of marine growth and hydrodynamic loading on offshore structures. *J Mek* 1996;1:77–98.

[88] Zeinoddini M, Bakhtiari A, Ehteshami M, Seif MS. Towards an understanding of the marine fouling effects on VIV of circular cylinders: response of cylinders with regular pyramidal roughness. *Appl Ocean Res* 2016;59:378–94. <http://dx.doi.org/10.1016/j.apor.2016.05.013>.

[89] Beech IB, Sunner JA, Hiraoka K. Microbe-surface interactions in biofouling and biocorrosion processes. *Int Microbiol* 2005;8:157–68. 16200494.

[90] Griffin OM. Vortex-induced vibrations of marine cables and structures. Washington DC: 1985.

[91] Jerez S, Trigo RM, Vicente-Serrano SM, Pozo-Vázquez D, Lorente-Plazas R, Lorenzo-Lacruz J, et al. The Impact of the North Atlantic Oscillation on Renewable Energy Resources in Southwestern Europe. *J Appl Meteorol Climatol* 2013;52:2204–25. <http://dx.doi.org/10.1175/JAMC-D-12-0257.1>.

[92] François B. Influence of winter North-Atlantic Oscillation on Climate-Related-Energy penetration in Europe. *Renew Energy* 2016;99:602–13. <http://dx.doi.org/10.1016/j.renene.2016.07.010>.

[93] Masselink G, Castelle B, Scott T, Dodet G, Suanez S, Jackson D, et al. Extreme wave activity during 2013/2014 winter and morphological impacts along the Atlantic coast of Europe. *Geophys Res Lett* 2016;43:2135–43. <http://dx.doi.org/10.1002/2015GL067492>.